

World Journal of *Clinical Cases*

World J Clin Cases 2021 November 16; 9(32): 9699-10051



REVIEW

- 9699 Emerging role of long noncoding RNAs in recurrent hepatocellular carcinoma
Fang Y, Yang Y, Li N, Zhang XL, Huang HF

MINIREVIEWS

- 9711 Current treatment strategies for patients with only peritoneal cytology positive stage IV gastric cancer
Bausys A, Gricius Z, Aniuksyte L, Luksta M, Bickaite K, Bausys R, Strupas K

ORIGINAL ARTICLE**Case Control Study**

- 9722 Botulinum toxin associated with fissurectomy and anoplasty for hypertonic chronic anal fissure: A case-control study
D'Orazio B, Geraci G, Famà F, Terranova G, Di Vita G
- 9731 Correlation between circulating endothelial cell level and acute respiratory distress syndrome in postoperative patients
Peng M, Yan QH, Gao Y, Zhang Z, Zhang Y, Wang YF, Wu HN

Retrospective Study

- 9741 Effects of early rehabilitation in improvement of paediatric burnt hands function
Zhou YQ, Zhou JY, Luo GX, Tan JL
- 9752 Intracortical screw insertion plus limited open reduction in treating type 31A3 irreducible intertrochanteric fractures in the elderly
Huang XW, Hong GQ, Zuo Q, Chen Q
- 9762 Treatment effects and periodontal status of chronic periodontitis after routine Er:YAG laser-assisted therapy
Gao YZ, Li Y, Chen SS, Feng B, Wang H, Wang Q
- 9770 Risk factors for occult metastasis detected by inflammation-based prognostic scores and tumor markers in biliary tract cancer
Hashimoto Y, Ajiki T, Yanagimoto H, Tsugawa D, Shinozaki K, Toyama H, Kido M, Fukumoto T
- 9783 Scapular bone grafting with allograft pin fixation for repair of bony Bankart lesions: A biomechanical study
Lu M, Li HP, Liu YJ, Shen XZ, Gao F, Hu B, Liu YF
- 9792 High-resolution computed tomography findings independently predict epidermal growth factor receptor mutation status in ground-glass nodular lung adenocarcinoma
Zhu P, Xu XJ, Zhang MM, Fan SF

- 9804** Colorectal cancer patients in a tertiary hospital in Indonesia: Prevalence of the younger population and associated factors

Makmun D, Simadibrata M, Abdullah M, Syam AF, Shatri H, Fauzi A, Renaldi K, Maulahela H, Utari AP, Pribadi RR, Muzellina VN, Nursyirwan SA

- 9815** Association between *Helicobacter pylori* infection and food-specific immunoglobulin G in Southwest China

Liu Y, Shuai P, Liu YP, Li DY

- 9825** Systemic immune inflammation index, ratio of lymphocytes to monocytes, lactate dehydrogenase and prognosis of diffuse large B-cell lymphoma patients

Wu XB, Hou SL, Liu H

Clinical Trials Study

- 9835** Evaluating the efficacy of endoscopic sphincterotomy on biliary-type sphincter of Oddi dysfunction: A retrospective clinical trial

Ren LK, Cai ZY, Ran X, Yang NH, Li XZ, Liu H, Wu CW, Zeng WY, Han M

Observational Study

- 9847** Management of pouch related symptoms in patients who underwent ileal pouch anal anastomosis surgery for adenomatous polyposis

Gilad O, Rosner G, Brazowski E, Kariv R, Gluck N, Strul H

- 9857** Presepsin as a biomarker for risk stratification for acute cholangitis in emergency department: A single-center study

Zhang HY, Lu ZQ, Wang GX, Xie MR, Li CS

Prospective Study

- 9869** Efficacy of Yiqi Jianpi anti-cancer prescription combined with chemotherapy in patients with colorectal cancer after operation

Li Z, Yin DF, Wang W, Zhang XW, Zhou LJ, Yang J

META-ANALYSIS

- 9878** Arthroplasty *vs* proximal femoral nails for unstable intertrochanteric femoral fractures in elderly patients: a systematic review and meta-analysis

Chen WH, Guo WX, Gao SH, Wei QS, Li ZQ, He W

CASE REPORT

- 9889** Synchronous multiple primary malignancies of the esophagus, stomach, and jejunum: A case report

Li Y, Ye LS, Hu B

- 9896** Idiopathic acute superior mesenteric venous thrombosis after renal transplantation: A case report

Zhang P, Li XJ, Guo RM, Hu KP, Xu SL, Liu B, Wang QL

- 9903** Next-generation sequencing technology for diagnosis and efficacy evaluation of a patient with visceral leishmaniasis: A case report

Lin ZN, Sun YC, Wang JP, Lai YL, Sheng LX

- 9911** Cerebral air embolism complicating transbronchial lung biopsy: A case report
Herout V, Brat K, Richter S, Cundrle Jr I
- 9917** Isolated synchronous Virchow lymph node metastasis of sigmoid cancer: A case report
Yang JQ, Shang L, Li LP, Jing HY, Dong KD, Jiao J, Ye CS, Ren HC, Xu QF, Huang P, Liu J
- 9926** Clinical presentation and management of drug-induced gingival overgrowth: A case series
Fang L, Tan BC
- 9935** Adult with mass burnt lime aspiration: A case report and literature review
Li XY, Hou HJ, Dai B, Tan W, Zhao HW
- 9942** Massive hemothorax due to intercostal arterial bleeding after percutaneous catheter removal in a multiple-trauma patient: A case report
Park C, Lee J
- 9948** Hemolymphangioma with multiple hemangiomas in liver of elderly woman with history of gynecological malignancy: A case report
Wang M, Liu HF, Zhang YZZ, Zou ZQ, Wu ZQ
- 9954** Rare location and drainage pattern of right pulmonary veins and aberrant right upper lobe bronchial branch: A case report
Wang FQ, Zhang R, Zhang HL, Mo YH, Zheng Y, Qiu GH, Wang Y
- 9960** Respiratory failure after scoliosis correction surgery in patients with Prader-Willi syndrome: Two case reports
Yoon JY, Park SH, Won YH
- 9970** Computed tomography-guided chemical renal sympathetic nerve modulation in the treatment of resistant hypertension: A case report
Luo G, Zhu JJ, Yao M, Xie KY
- 9977** Large focal nodular hyperplasia is unresponsive to arterial embolization: A case report
Ren H, Gao YJ, Ma XM, Zhou ST
- 9982** Fine-needle aspiration cytology of an intrathyroidal nodule diagnosed as squamous cell carcinoma: A case report
Yu JY, Zhang Y, Wang Z
- 9990** Extensive abdominal lymphangiomatosis involving the small bowel mesentery: A case report
Alhasan AS, Daqqaq TS
- 9997** Gastrointestinal symptoms as the first sign of chronic granulomatous disease in a neonate: A case report
Meng EY, Wang ZM, Lei B, Shang LH
- 10006** Screw penetration of the iliopsoas muscle causing late-onset pain after total hip arthroplasty: A case report
Park HS, Lee SH, Cho HM, Choi HB, Jo S

- 10013** Uretero-lumbar artery fistula: A case report
Chen JJ, Wang J, Zheng QG, Sun ZH, Li JC, Xu ZL, Huang XJ
- 10018** Rare mutation in *MKRN3* in two twin sisters with central precocious puberty: Two case reports
Jiang LQ, Zhou YQ, Yuan K, Zhu JF, Fang YL, Wang CL
- 10024** Primary mucosal-associated lymphoid tissue extranodal marginal zone lymphoma of the bladder from an imaging perspective: A case report
Jiang ZZ, Zheng YY, Hou CL, Liu XT
- 10033** Focal intramural hematoma as a potential pitfall for iatrogenic aortic dissection during subclavian artery stenting: A case report
Zhang Y, Wang JW, Jin G, Liang B, Li X, Yang YT, Zhan QL
- 10040** Ventricular tachycardia originating from the His bundle: A case report
Zhang LY, Dong SJ, Yu HJ, Chu YJ
- 10046** Posthepatectomy jaundice induced by paroxysmal nocturnal hemoglobinuria: A case report
Liang HY, Xie XD, Jing GX, Wang M, Yu Y, Cui JF

ABOUT COVER

Editorial Board Member of *World Journal of Clinical Cases*, Jalaj Garg, FACC, MD, Academic Research, Assistant Professor, Division of Cardiology, Medical College of Wisconsin, Milwaukee, WI 53226, United States.
garg.jalaj@yahoo.com

AIMS AND SCOPE

The primary aim of *World Journal of Clinical Cases (WJCC, World J Clin Cases)* is to provide scholars and readers from various fields of clinical medicine with a platform to publish high-quality clinical research articles and communicate their research findings online.

WJCC mainly publishes articles reporting research results and findings obtained in the field of clinical medicine and covering a wide range of topics, including case control studies, retrospective cohort studies, retrospective studies, clinical trials studies, observational studies, prospective studies, randomized controlled trials, randomized clinical trials, systematic reviews, meta-analysis, and case reports.

INDEXING/ABSTRACTING

The *WJCC* is now indexed in Science Citation Index Expanded (also known as SciSearch®), Journal Citation Reports/Science Edition, Scopus, PubMed, and PubMed Central. The 2021 Edition of Journal Citation Reports® cites the 2020 impact factor (IF) for *WJCC* as 1.337; IF without journal self cites: 1.301; 5-year IF: 1.742; Journal Citation Indicator: 0.33; Ranking: 119 among 169 journals in medicine, general and internal; and Quartile category: Q3. The *WJCC*'s CiteScore for 2020 is 0.8 and Scopus CiteScore rank 2020: General Medicine is 493/793.

RESPONSIBLE EDITORS FOR THIS ISSUE

Production Editor: Jia-Hui Li; Production Department Director: Yu-Jie Ma; Editorial Office Director: Jin-Lai Wang.

NAME OF JOURNAL

World Journal of Clinical Cases

ISSN

ISSN 2307-8960 (online)

LAUNCH DATE

April 16, 2013

FREQUENCY

Thrice Monthly

EDITORS-IN-CHIEF

Dennis A Bloomfield, Sandro Vento, Bao-Gan Peng

EDITORIAL BOARD MEMBERS

<https://www.wjgnet.com/2307-8960/editorialboard.htm>

PUBLICATION DATE

November 16, 2021

COPYRIGHT

© 2021 Baishideng Publishing Group Inc

INSTRUCTIONS TO AUTHORS

<https://www.wjgnet.com/bpg/gerinfo/204>

GUIDELINES FOR ETHICS DOCUMENTS

<https://www.wjgnet.com/bpg/GerInfo/287>

GUIDELINES FOR NON-NATIVE SPEAKERS OF ENGLISH

<https://www.wjgnet.com/bpg/gerinfo/240>

PUBLICATION ETHICS

<https://www.wjgnet.com/bpg/GerInfo/288>

PUBLICATION MISCONDUCT

<https://www.wjgnet.com/bpg/gerinfo/208>

ARTICLE PROCESSING CHARGE

<https://www.wjgnet.com/bpg/gerinfo/242>

STEPS FOR SUBMITTING MANUSCRIPTS

<https://www.wjgnet.com/bpg/GerInfo/239>

ONLINE SUBMISSION

<https://www.f6publishing.com>

Retrospective Study

High-resolution computed tomography findings independently predict epidermal growth factor receptor mutation status in ground-glass nodular lung adenocarcinoma

Ping Zhu, Xiao-Jun Xu, Min-Ming Zhang, Shu-Feng Fan

ORCID number: Ping Zhu 0000-0002-7416-2278; Xiao-Jun Xu 0000-0002-0127-2812; Min-Ming Zhang 0000-0003-0145-7558; Shu-Feng Fan 0000-0003-1365-986X.

Author contributions: Zhu P contributed to literature research, clinical studies, statistical analysis, manuscript preparation and editing; Xu XJ contributed to experimental studies/data analysis; Zhang MM was the guarantor of integrity of the entire study; Fan SF contributed to study concepts and design; all authors have read and approved the final manuscript.

Institutional review board

statement: This study was approved by the Ethics Committee of the Second Affiliated Hospital of Zhejiang Chinese Medical University, Zhejiang Province, China.

Informed consent statement: The individual consent was waived by the committee owing to the retrospective study design.

Conflict-of-interest statement: We have no financial relationships to disclose.

Data sharing statement: The data

Ping Zhu, Xiao-Jun Xu, Min-Ming Zhang, Shu-Feng Fan, Department of Radiology, The Second Affiliated Hospital of Zhejiang Chinese Medical University, Hangzhou 310005, Zhejiang Province, China

Corresponding author: Shu-Feng Fan, PhD, Doctor, Department of Radiology, The Second Affiliated Hospital of Zhejiang Chinese Medical University, No. 318 Chaowang Road, Gongshu District, Hangzhou 310005, Zhejiang Province, China. shufengfan16@126.com

Abstract

BACKGROUND

For lung adenocarcinoma with epidermal growth factor receptor (EGFR) gene mutation, small molecule tyrosine kinase inhibitors are more effective. Some patients could not obtain enough histological specimens for EGFR gene mutation detection. Specific imaging features can predict EGFR mutation status to a certain extent.

AIM

To assess the associations of EGFR mutations with high-resolution computerized tomography (HRCT) features in ground-glass nodular lung adenocarcinoma.

METHODS

This study retrospectively assessed patients with ground-glass nodular lung adenocarcinoma diagnosed between January 2011 and March 2017. EGFR gene mutations in exons 18-21 were detected. The patients were classified into mutant EGFR and wild-type groups, and general data and HRCT image characteristics were assessed.

RESULTS

Among 98 patients, 31 (31.6%) and 67 (68.4%) had mutated and wild-type EGFR in exons 18-21, respectively. Gender, age, smoking history, location of lesions, morphology, edges, borders, pleural indentations, and associations of nodules with bronchus and blood vessels were comparable in both groups (all $P > 0.05$). Patients with mutant EGFR had larger nodules than those with the wild-type (17.19 ± 6.79 and 14.37 ± 6.30 mm, respectively; $P = 0.047$). Meanwhile, the vacuole/honeycomb sign was more frequent in the mutant EGFR group ($P = 0.011$). The logistic regression prediction model included the combination of

set supporting the results of this article are included within the article.

Supported by the Zhejiang Province Traditional Chinese Medicine Science and Technology Plan - Zhejiang Province Traditional Chinese Medicine Project for Traditional Chinese Medicine Scientific Research (2020) (Class B), No. 2020ZB117.

Country/Territory of origin: China

Specialty type: Medicine, research and experimental

Peer-review report's scientific quality classification

Grade A (Excellent): 0
Grade B (Very good): B, B
Grade C (Good): 0
Grade D (Fair): 0
Grade E (Poor): 0

Open-Access: This article is an open-access article that was selected by an in-house editor and fully peer-reviewed by external reviewers. It is distributed in accordance with the Creative Commons Attribution NonCommercial (CC BY-NC 4.0) license, which permits others to distribute, remix, adapt, build upon this work non-commercially, and license their derivative works on different terms, provided the original work is properly cited and the use is non-commercial. See: <http://creativecommons.org/licenses/by-nc/4.0/>

Received: June 4, 2021

Peer-review started: June 4, 2021

First decision: June 25, 2021

Revised: July 30, 2021

Accepted: September 22, 2021

Article in press: September 22, 2021

Published online: November 16, 2021

P-Reviewer: Sugimura H, Tahtabasi M

S-Editor: Wang LL

L-Editor: A

P-Editor: Ma YJ



nodule size and vacuole/honeycomb sign (OR = 1.120, 95%CI: 1.023-1.227, $P = 0.014$) revealed a sensitivity of 83.9%, a specificity of 52.2% and an AUC of 0.698 (95%CI: 0.589-0.806; $P = 0.002$).

CONCLUSION

Nodule size and vacuole/honeycomb features could independently predict EGFR mutation status in ground-glass nodular lung adenocarcinoma.

Key Words: Lung adenocarcinoma; Tomography; Epidermal growth factor receptor; Logistic model; Receiver operating characteristic analysis

©The Author(s) 2021. Published by Baishideng Publishing Group Inc. All rights reserved.

Core Tip: For patients who have been clinically diagnosed with lung adenocarcinoma but failed to undergo epidermal growth factor receptor (EGFR) gene testing: When the lesion is shown as a pure ground glass nodule, and the size of the nodule is ≥ 8.65 mm, it can be used as an independent indicator to predict EGFR gene mutation. The appearance of the vesicle sign or honeycomb sign may indicate a mutation in the EGFR gene.

Citation: Zhu P, Xu XJ, Zhang MM, Fan SF. High-resolution computed tomography findings independently predict epidermal growth factor receptor mutation status in ground-glass nodular lung adenocarcinoma. *World J Clin Cases* 2021; 9(32): 9792-9803

URL: <https://www.wjgnet.com/2307-8960/full/v9/i32/9792.htm>

DOI: <https://dx.doi.org/10.12998/wjcc.v9.i32.9792>

INTRODUCTION

Lung cancer is the deadliest malignancy worldwide, with a mortality of 1.59 million cases recorded in 2012[1]. Non-small cell lung cancer (NSCLC) represents the commonest histopathological subtype, accounting for up to 85% of all lung cancer cases[2]. Although small cell lung cancer occurs less frequently, it shows higher aggressiveness compared with NSCLC[3]. In recent years, with tremendous progress in molecular cell biology, the treatment of advanced NSCLC is mainly focused on targeted drug delivery[4-6]. The majority of patients with NSCLC show epidermal growth factor receptor (EGFR) mutations, especially in the East Asian population[7]. The discovery of EGFR mutations and the corresponding tyrosine kinase inhibitors (TKIs) has markedly improved prognosis in EGFR-positive lung cancer. Currently, multiple EGFR TKIs, including afatinib, erlotinib, and gefitinib, are widely applied in NSCLC therapy, particularly in cases with exon 19 deletions and exon 21 substitutions of the EGFR gene[8]. Interestingly, Yatabe *et al*[9] demonstrated that EGFR mutations play an important role in the progression from atypical adenomatoid hyperplasia to adenocarcinoma *in situ*, then to minimally invasive adenocarcinoma, and finally to invasive pulmonary adenocarcinoma in lung adenocarcinoma. Meanwhile, a number of studies have shown significant correlations between EGFR mutations and the therapeutic effects of molecular-targeted drugs[10-12].

An optimal treatment strategy for NSCLC involves the screening of tumors for predictive and prognostic biomarkers, which could predict sensitivity to targeted therapeutics and estimate prognosis, respectively[13]. Patients are often tested for genetic mutations in tissue samples before therapy, which requires a biopsy, which is invasive, expensive, and time-consuming[14,15]. In addition, different histological heterogeneity patterns observed in the same tumor may lead to false-negative results [14,15]. Therefore, non-invasive methods to predict EGFR mutations are of high importance but currently lacking. A study reported electric field-induced release and measurement as an effective, accurate, rapid, user-friendly, and cost-effective tool for detecting EGFR mutations in the saliva of NSCLC cases; however, this study did not assess other uncommon EGFR-TKI sensitive mutations[16].

Applying high-resolution computerized tomography (HRCT) for lung cancer screening, previous studies have shown that certain imaging characteristics could

predict EGFR mutation status to a certain extent[17,18]. However, the value of HRCT in predicting EGFR mutations remains unclear. Therefore, this study aimed to assess the associations of EGFR mutations with HRCT features in ground-glass nodular lung adenocarcinoma.

MATERIALS AND METHODS

Patients

This retrospective study included lung adenocarcinoma patients with one or two ground-glass nodules (GGNs) on chest HRCT who were admitted to the Department of Thoracic Surgery of the Second Affiliated Hospital of Zhejiang Chinese Medical University from January 2011 to March 2017. The patients underwent pulmonary wedge resection, segmental resection, or lobectomy in the Department of Thoracic Surgery. EGFR mutation status was detected after surgery, and the patients were classified into the mutant EGFR and wild-type groups.

The inclusion criteria were as follows: (1) A clinical diagnosis of lung adenocarcinoma, confirmed by postoperative pathology; (2) A complete set of HRCT images in the picture archiving and communication system; (3) One or two GGNs (pure or partially solid) in lungs on HRCT with a layer thickness of ≤ 1.5 mm; and (4) Intrapulmonary nodules with a maximum diameter of ≤ 3 cm.

The exclusion criteria were: (1) Diffuse GGNs in the lung; or (2) Incomplete medical records.

This study was approved by the Ethics Committee of the Second Affiliated Hospital of Zhejiang Chinese Medical University, Zhejiang, China, with a waiver for individual consent by the committee owing to the retrospective study design.

CT scan examination

Before CT scanning, all patients were trained to breathe. All patients underwent chest CT scanning at full inspiration in the supine position. The scanning range encompassed the entire area from the apex to the base of the lungs, including the axilla and chest wall of both sides.

The scans were performed on a Somatom Sensation 16 CT Scanner (Siemens, Germany), GE Light speed RT16 (GE, United States), Somatom Definition AS (Siemens), Aquilion ONE 320 (Toshiba, Japan), or GE Optima CT540 (GE). Plain and enhanced CT scans were performed at a tube voltage of 120 kVp and a tube current of 140 mAs; screw pitches were 1.2 and 1.45, and the rack rotation time was 0.5 s/rev. A non-ionic contrast agent was administered at a dose of 300 mgI/mL (100 mL) by injection *via* the cubital vein at 2.5 mL/s with a pressure syringe. Scanning was initiated after a delay of 28 s. High-resolution reconstruction was performed with layer thickness and interval of 1.25 mm and 0.625 mm, respectively; layer thickness and interval of 1.5 mm and 1.0 mm, respectively; or layer thickness of 2.0 mm and interval 1.25 mm, respectively. Multiplanar reformation reconstruction was conducted to show the relationship and morphology of the lesions and adjacent structures.

Two radiologists with more than 10 years of experience who were blinded to the gene mutation data read the CT scans and analyzed the characteristics of HRCT images independently. In case of discrepancy, the data were examined by a chief physician with more than 20 years of experience.

All nodules were assessed under the lung window (position, -700 Hu; width, 1500 Hu)[19]. GGNs were defined as increased density and focal cloud-like density shadows on CT images, but with a density not sufficient to cover the bronchial vascular bundle passing through them[20]. The mediastinum window was set as follows: position, 20 Hu; width, 400 Hu. Lesions were classified into pure and partially-solid GGNs according to whether they contained solid components[21]. Pure GGNs were defined as increased focal pure ground glass-like density in the lung parenchyma, with normal structures such as the edge contours of blood vessels in the lesion still clearly visible. No solid components were observed in the mediastinum window, and vascular approach shadows were excluded. Partially solid GGNs were defined as increased density attenuation value in the lesion area, with some normal structures such as the edge contours of blood vessels completely covered, while others remained clearly visible.

Pathological tissue examination and genetic testing

All nodules were resected by thoracotomy or thoracoscopy. Conventional paraffin-embedded sections, HE staining, and quantitative PCR ($M \times 3000p$ qPCR system,

Agilent Technologies, Inc., Santa Clara, CA, United States) were used to detect the mutation status of the EGFR gene. The kits for DNA extraction (Cat. No # 8.02.23501X036G) and EGFR mutation detection (Cat. No # 8.01.20201W012A) were manufactured by Amoy Diagnostics Co., Ltd. (AmoyDx, China). Any discrepancy was resolved by discussion until the two pathologists reached a consensus.

Data collection

Demographic and clinical data of patients were collected, including age, gender, smoking history, nodular properties, histopathological diagnosis, and lesion location.

Image analyses

For pure GGNs, the layer with the largest lesion was selected, and the longest and short (perpendicular to the longest diameter) diameters were measured[22].

Size of the lesion = (longest diameter + short diameter) / 2.

For partially solid nodules, the lesion size (the same as for pure GGNs) and the proportion of components were measured, respectively.

Proportion of solid component = the longest diameter of solid component / lesion size.

Proportion of ground-glass component = 1-proportion of the solid component.

Morphology (round-like/ovoid or irregular), margin (with or without spicule), border (lobular or not), inner character (with or without vacuole/honeycomb sign), and relationships of GGNs with the bronchus and blood vessels were also assessed (Figure 1). Relationships with the bronchus were classified as follows: (1) Bronchus truncated in the nodule; (2) Bronchus continuous in the nodule and twisted or dilated; (3) Bronchus normally continuous in the nodule, without dilation or twist; or (4) Bronchus with no relationship with ground-glass shadows. Either (2) or (3) indicated air bronchogram sign. Relationships with blood vessels were classified as follows: (1) Blood vessels closely packed around the nodule, with an adherent-like pattern; (2) Blood vessels closely packed within the nodule; or (3) Vascular clustering sign around the nodule.

Statistical analyses

Statistical analyses were performed using the SPSS statistical software (version 19.0, IBM, Armonk, NY, United States). Continuous variables were expressed as mean \pm SD. Comparisons between groups were performed by independent samples *t*-test or the Mann-Whitney U-test. Categorical variables were expressed as frequency and percentage and compared by Pearson's chi-square test or the Fisher's exact probability method. A predictive model was constructed with the Logistic regression model, and receiver operating characteristic (ROC) curve analysis was performed to determine the sensitivity, specificity, and area under the curve (AUC). $P < 0.05$ was considered statistically significant.

RESULTS

Patient baseline characteristics

There were 98 patients in this study, aged 32 to 85 years (average age of 64.24 ± 14.65 years). They included 31 cases (12 males and 19 females) in the mutant group, with an average age of 66.6 ± 14.2 years, and 67 cases (30 males and 37 females) in the wild-type group, with an average age of 62.7 ± 15.6 years. Eight (25.81%) and 24 (35.82%) patients had a history of smoking in the mutant and wild-type groups, respectively. There were 7 (22.58%) and 24 (77.42%) cases of pure and partially-solid nodules in the mutant group, respectively; meanwhile, 21 (31.34%) and 46 (68.66%) cases of pure and partially-solid nodules were found in the wild-type group. There were no significant differences in baseline characteristics between the two groups (all $P > 0.05$) (Table 1).

HRCT signs

HRCT signs are summarized in Table 2. Nodule sizes were 17.19 ± 6.79 and 14.37 ± 6.30 mm in the mutant and wild-type groups, respectively ($P = 0.047$), indicating a statistically significant difference. For pure GGNs, the mutant group showed significantly larger lesions compared with the wild-type group (12.79 ± 5.24 vs 9.24 ± 3.26 mm; $P = 0.042$). However, partially-solid nodules showed no statistically significant differences in nodule size (18.63 ± 6.47 vs 16.68 ± 6.05 mm, $P = 0.216$) and proportion of ground-glass component ($56.10 \pm 24.01\%$ vs $51.05 \pm 28.13\%$, $P = 0.457$).

Table 1 Baseline and clinical characteristics

	Mutant EGFR group (n = 31)	Wild-type group (n = 67)	P value
Age (yr)	66.6 ± 14.2	62.7 ± 15.6	0.221
< 60	13 (41.9%)	37 (55.2%)	
≥ 60	18 (58.1%)	30 (44.8%)	
Male	12 (38.7%)	30 (44.8%)	0.573
Smoking history	8 (25.8%)	24 (35.8%)	0.326
Nodule property			0.372
Pure GGNs	7 (22.6%)	21 (31.3%)	
Partial solid nodules	24 (77.4%)	46 (68.7%)	
Histopathologic diagnosis			0.723
Preinvasive lesions (AAH + AIS)	5 (16.1%)	9 (13.4%)	
Invasive lesions (MIA + IPA)	26 (83.9%)	58 (86.6%)	
Position of the nodule			0.471
Right upper lobe	10 (32.3%)	27 (40.3%)	
Right middle lobe	4 (12.9%)	8 (11.9%)	
Right lower lobe	6 (19.4%)	9 (13.4%)	
Left upper lobe	5 (16.1%)	17 (25.4%)	
Left lower lobe	6 (19.4%)	6 (9.0%)	
Time between CT scan and surgery (days)	7.0 (4.5, 13.5)	8.0 (6.0, 13.0)	0.545

EGFR: Epidermal growth factor receptor; GGN: Ground-glass nodule; AAH: atypical adenomatoid hyperplasia; AIS: adenocarcinoma *in situ*; MIA: minimally invasive adenocarcinoma; IPA: invasive pulmonary adenocarcinoma.

between the mutant and wild-type groups.

The occurrence rate of the vacuole/honeycomb sign was significantly higher in the mutant group compared with the wild-type group (80.6% *vs* 53.7%, $P = 0.011$).

The remaining indexes assessed showed no differences between the two groups, including nodule morphology, spicule presence or absence on the nodule edge, presence or absence of lobular borders, presence or absence of pleural indentation, relationship with the bronchus (air bronchogram), and relationship with blood vessels (vascular bundle sign) (all $P > 0.05$).

Logistic regression analysis for the presence of EGFR mutations

The logistic regression analyses showed that the nodule size was independently associated with EGFR mutations (OR = 1.068, 95%CI: 1.000-1.141, $P = 0.049$), while the combination of nodule size with vacuole/honeycomb sign (OR = 1.120, 95%CI: 1.023-1.227, $P = 0.014$) was also independently associated with EGFR mutations (Table 3).

Predictive values of nodule size and vacuole/honeycomb sign in determining EGFR mutation status

ROC curve analysis was performed to determine the value of nodule size alone or in combination with vacuole/honeycomb sign in predicting EGFR mutation status. For pure ground-glass nodular lung adenocarcinoma, an optimal cut-off value between the mutant and wild-type groups of 8.65 mm was found. Lesions ≥ 8.65 mm in size were determined to be EGFR mutant, with a sensitivity of 100%, a specificity of 57.1%, and an AUC of 0.782 (95%CI:0.609-0.956; $P = 0.028$) (Figure 2A). For all ground-glass nodular tumors, nodule size at a cut-off of 13.38 mm yielded sensitivity, specificity, and AUC of 74.2%, 50.7%, and 0.625 (95%CI: 0.504-0.745; $P = 0.048$), respectively. Vacuole or honeycomb sign was significantly associated with EGFR mutation. Therefore, we next evaluated nodule size in combination with vacuole/honeycomb sign in predicting EGFR mutation status, and a sensitivity of 83.9%, a specificity of 52.2%, and an AUC of 0.698 (95%CI: 0.589-0.806, $P = 0.002$) were obtained (Table 4 and Figure 2B).

Table 2 High-resolution computerized tomography signs

HRCT findings	Mutant EGFR group (n = 31)	Wild-type group (n = 67)	P value
Nodule size (mm)	17.19 ± 6.79	14.37 ± 6.30	0.047 ^a
Pure GGNs			
Nodule size (mm)	12.79 ± 5.24	9.24 ± 3.26	0.042 ^a
Partial solid nodules			
Nodule size (mm)	18.63 ± 6.47	16.68 ± 6.05	0.216
Proportion of ground-glass component (%)	56.10 ± 24.01	51.05 ± 28.13	0.457
Nodule morphology			0.137
Round-like/ovoid	14 (45.2%)	41 (61.2%)	
Irregular	17 (54.8%)	26 (38.8%)	
Spicules on the edge of the nodule	20 (64.5%)	34 (50.7%)	0.202
Lobules on the border of the nodule	29 (93.5%)	61 (91.0%)	1.000
Vacuole/honeycomb sign	25 (80.6%)	36 (53.7%)	0.011 ^a
Pleural indentation	20 (64.5%)	33 (49.3%)	0.159
Relationship with bronchus/bronchovascular bundles			0.613
Bronchus truncated in the nodule	1 (3.2%)	6 (9.0%)	
Bronchus continuous in the nodule, with dilation or twisted appearance	11 (35.5%)	20 (29.9%)	
Bronchus continuous in the nodule, without dilation or twisted appearance	7 (22.6%)	11 (16.4%)	
Bronchus not associated with ground-glass shadows	12 (38.7%)	30 (44.8%)	
Relationship with blood vessels			0.488
Blood vessels closely packed around the nodule with adherent-like pattern	0 (0.0%)	3 (4.5%)	
Blood vessels closely packed within the nodule	20 (64.5%)	41 (61.2%)	
Vascular clustering around the nodule	11 (35.5%)	23 (34.3%)	

^aP < 0.05 is statistically significant.

HRCT: high-resolution computerized tomography; EGFR: Epidermal growth factor receptor; GGN: ground-glass nodule.

Table 3 Logistic regression analysis for the presence of epidermal growth factor receptor mutations

Variables	OR	95%CI	P value
Nodule size	1.068	1.000-1.141	0.049 ^a
Nodule size + vacuole/honeycomb sign	1.120	1.023-1.227	0.014 ^a

^aP < 0.05 is statistically significant.

DISCUSSION

The current study demonstrated that HRCT characteristics, including nodule size and vacuole/honeycomb sign, could predict EGFR mutation status in ground-glass nodular lung adenocarcinoma.

This study showed that on HRCT images, there were no statistically significant differences in signs, including lesion morphology, spicule sign, lobulation sign, pleural indentation, air bronchogram, and vascular bundle sign between the mutant EGFR and wild-type groups. Different from our results, Hasegawa *et al*[23] assessed the HRCT signs in 263 patients with lung adenocarcinoma based on EGFR mutation status, and EGFR mutations were more common in cases with vascular convergence sign, pleural indentation, bilateral multiple lung metastases, and ground-glass components in the lesions. In addition, a model for predicting EGFR mutation status

Table 4 Area under the receiver operating characteristic curve of the models

Model	AUC	SE	95%CI	P value
Nodule size	0.625	0.061	0.504–0.745	0.048 ^a
Nodule size + vacuole/honeycomb sign	0.698	0.055	0.589–0.806	0.002 ^a

^a $P < 0.05$ is statistically significant.

ROC: receiver operating characteristic; AUC: area under the curve; SE: standard error; CI: confidence interval.

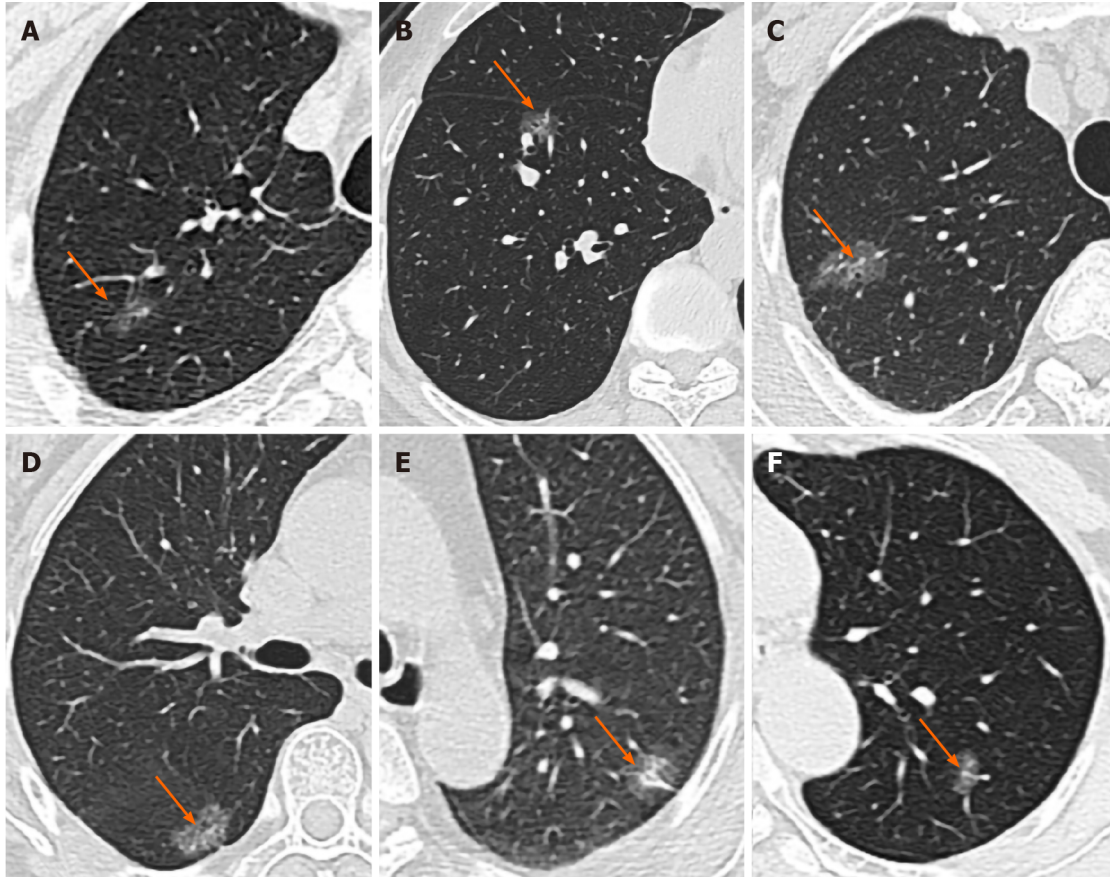


Figure 1 High-resolution computed tomography images. A: An irregularly shaped pure ground-glass nodule (GGN, arrow) in the right lower lobe. Vacuole sign was seen inside the lesion, and the overall tumor size was about 10 mm, which was consistent with a minimally invasive adenocarcinoma (MIA) that harbored epidermal growth factor receptor (EGFR) exon 21 L858R compound mutation; B: A round-like GGN (arrow) located in the right upper lobe with a diameter of 14 mm, which strongly suggested an MIA that harbored EGFR exon 21 L858R compound mutation. Visceral pleural invasion with honeycomb signs were also seen; C: An irregularly shaped GGN (arrow) in the right middle lobe with a diameter of approximately 22 mm, which was consistent with invasive pulmonary adenocarcinoma (IPA) that harbored EGFR exon 19 deletion. Vacuole sign was seen inside the lesion; D: An ovoid GGN (arrow) in the right lower lobe with a diameter of about 16 mm, which indicated IPA that harbored EGFR exon 21 L858R compound mutation. Honeycomb sign was seen inside; E: Female, 64 years old. A partially solid circular nodules was seen in the upper lobe of the left lung, about 17 mm in diameter, showing as superficial lobulated nodules. The pleura was locally pulled. The wild type of the IPA and EGFR genes was confirmed by pathology; F: Female, 58 years old. An irregular, partially solid nodule was found in the upper lobe of the left lung, about 11 mm in diameter, showing as superficial lobulated nodules. One vessel extended into the lesion and thickened. The wild type of the IPA and EGFR genes was confirmed by pathology.

was constructed, with an AUC of 0.79, a sensitivity of 78.4%, and a specificity of 70.4% [23]. The main pathological basis for the formation of pleural indentation includes fibrous tissue hyperplasia and scar formation in the tumor, connective tissue thickening, and reactive fibrous hyperplasia around the lesion; this leads to pleural contraction, which is a common sign of visceral pleural invasion. Vessel convergence sign indicates fibrous tissue hyperplasia and scar formation in the tumor, invasive growth towards blood vessels, and pulling of adjacent blood vessels to shift to the tumor. Both signs suggest a high degree of malignancy. However, the currently available data regarding its associations with EGFR mutations are quite divergent[17, 24], and further research is expected.

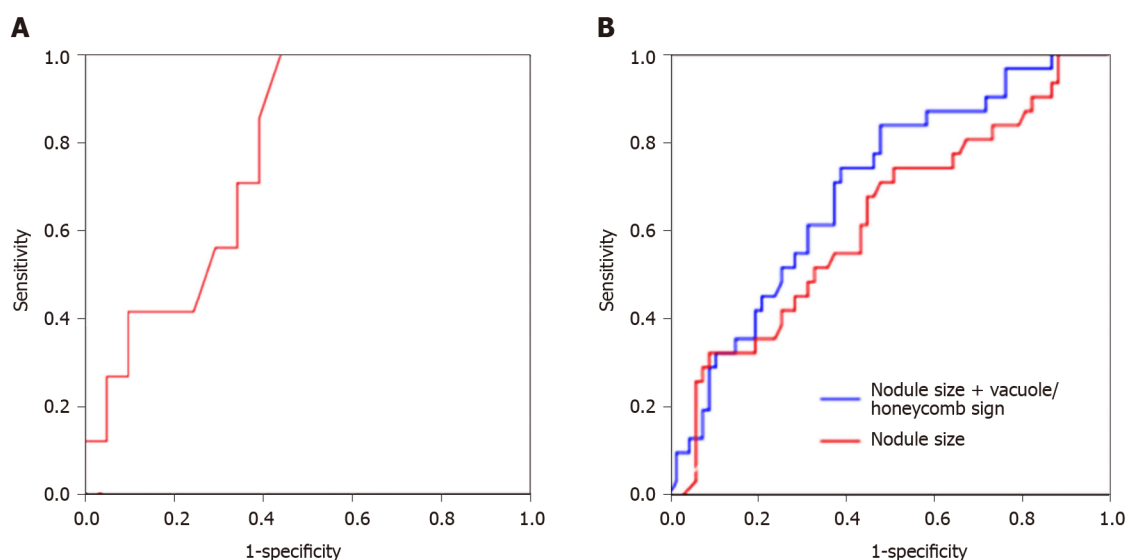


Figure 2 Receiver operating characteristic curves. A: Receiver operating characteristic curves for assessing the predictive values of nodule size (red). For pure ground-glass nodular adenocarcinomas with epidermal growth factor receptor (EGFR) mutations, the optimal cut-off value was 8.65 mm; the model yielded a sensitivity of 100%, a specificity of 57.1%, and an AUC of 0.782 (95%CI: 0.609–0.956; $P = 0.028$); B: Nodule size (red) and nodule size in combination with vacuole/honeycomb sign (blue) in ground-glass nodular adenocarcinomas (mixed) with EGFR mutations. The optimal cutoff value was set to 13.38 mm; the sensitivity, specificity and AUC were 74.2%, 50.7%, and 0.625 (95%CI: 0.504-0.745; $P = 0.048$), respectively. The final model showed an AUC of 0.698 (95%CI: 0.589-0.806; $P = 0.002$). Its sensitivity was 83.9% and specificity was 52.2%.

Air bronchogram is due to tumor cells growing along the bronchiolar wall in a mural-like manner, with non-damaged supporting structures of the lung and long or branched low-density shadows observed in or around the tumor on continuous layers. Dai *et al*[25] retrospectively analyzed 204 patients with pathologically confirmed stage I lung adenocarcinoma and found that air bronchogram is more common in patients with positive EGFR mutations. They concluded that an air bronchogram could be used as an independent predictor of EGFR mutations in lung adenocarcinoma. In this study, however, there was no statistically significant difference in air bronchogram between the EGFR mutation and wild-type groups. The differences observed in our study could be partly attributed to low statistical power due to the small sample size of the mutant EGFR group. Another possible explanation could be the differences in patient selection resulting in an inherent selection bias in our study population.

One of the main findings of this study is that lesion size was an independent predictor of EGFR mutation status. Using the criterion of nodule size ≥ 8.65 mm to predict the occurrence of EGFR gene mutation, a sensitivity as high as 100% was obtained. Multiple studies have reported significant associations between tumor size and EGFR mutation in lung adenocarcinoma[26-28]. However, nodule size was not consistently found to be a significant factor in some other studies[28,29]. Further studies with a large sample size are warranted to confirm this finding.

A study by Hong *et al*[29] showed that tumors containing any proportion of GGO have a significantly higher rate of EGFR mutations than those without GGO components. Yano *et al*[24] evaluated 80 peripheral lung cancer cases and found that GGO components $> 50\%$ could be used as an indicator to predict EGFR gene mutation. This indicated that the ground-glass component in nodules plays an important role in predicting EGFR mutations status. The current study showed that in patients with confirmed lung adenocarcinoma, EGFR mutations certainly occurred when the lesion size was ≥ 8.65 mm. For lesions showing mixed GGNs, with an average ground-glass component in the lesion $> 50\%$, there was no significant difference between the mutant and wild groups. Nevertheless, different from previous studies, we only included patients with GGNs, and those with solid nodules were excluded. The difference in patient selection, as well as the small sample size, may lead to different results.

Another interesting finding of this study is that the HRCT feature, vacuole/honeycomb sign occurred more frequently in the mutant EGFR group than the wild-type group. GGNs usually appear as pseudovoids, where tumors infiltrate along the tube wall to form a valve-like obstruction in the lumen. Consequently, the increase in lung density is the result of the replacement of air in the alveoli by fluid, cells, or fibrosis, causing the alveolar cavity to overinflate, which then manifested as GGNs in small vacuoles[30]. However, the vacuole/honeycomb sign was not commonly

observed in previous studies, and further research is in need to verify this finding.

Notably, the median time between CT scan and resection surgery was 7.0 and 8.0 days for mutant EGFR and wild-type groups, respectively, with no statistically significant difference between the two groups. Despite the fact that the passage of time may result in an increase in the size of most malignant nodules, predicting the EGFR mutation status by nodule size alone may not be reliable. Therefore, this finding might suggest that nodule size in combination with other CT features such as the vacuole/honeycomb sign could be a better predictor. Given the prolonged volume doubling time of the lesion[31,32] and the short time interval in this study, the altered diameter and volume of the lesion may not be significant enough to influence the prediction of EGFR status.

The limitations of this study should be mentioned. First, this was a single-center study with a small sample size, which may cause some CT signs to be not statistically significant, and associations of lung adenocarcinoma subtypes with EGFR gene mutations or HRCT positive, EGFR negative with rare EGFR mutations could not be assessed. Secondly, due to the non-availability of suitable measurement software in our hospital, the volumes of GGNs were not analyzed in this study. Thirdly, the time interval between CT examination and surgery was large in a few cases, which might limit the generalizability of conclusions from our study. Fourthly, survival analysis was not performed. Finally, this paper examined the EGFR status in patients with ground-glass nodular lung adenocarcinoma, but there was no control group. Therefore, in future work, we will collect data about the elderly (> 60 years of age), smoking men compared with middle-aged women (40-60 years old), and never-smoking women to explore whether there are differences in HRCT signs between the two. As for the regional problem, our group can only collect data from Asian patients, but multicenter international studies could address this issue. Still, such studies will have to be carefully designed since scanners with a lower resolution might miss some features of EGFR mutations. International guidelines suggest that low-dose spiral CT screening should be carried out in high-risk groups[22,33-35]. Still, low-dose CT is only suitable for routine screening in high-risk groups. Once suspicious lesions are found during screening, routine HRCT examination should be performed to enable a more detailed assessment of lesions[22,33-35]. The present study only included patients who underwent HRCT as confirmation of regular lung cancer screening. Therefore, studies with larger sample sizes are warranted, and factors such as CT value, volume of GGNs, and lung adenocarcinoma subtype would be included to develop a more comprehensive and accurate model for predicting the mutation status of the EGFR gene, to provide a basis for clinical decision-making.

CONCLUSION

In conclusion, HRCT signs were associated with EGFR mutation status in lung adenocarcinoma, and nodule size combined with vacuole/honeycomb sign could predict EGFR mutation status to a certain extent. Future studies are warranted to confirm these findings and improve the non-invasive detection of EGFR gene mutations in lung cancer.

ARTICLE HIGHLIGHTS

Research background

Applying high-resolution computerized tomography (HRCT) for lung cancer screening, previous studies have shown that certain imaging characteristics could predict epidermal growth factor receptor (EGFR) mutation status to a certain extent.

Research motivation

Non-invasive methods to predict EGFR mutations are of high importance but currently lacking. The value of HRCT in predicting EGFR mutations remains unclear.

Research objectives

This study aimed to assess the associations of EGFR mutations with HRCT features in ground-glass nodular lung adenocarcinoma.

Research methods

This study retrospectively assessed patients with ground-glass nodular lung adenocarcinoma diagnosed between January 2011 and March 2017. EGFR gene mutations in exons 18-21 were detected. The patients were classified into mutant EGFR and wild-type groups, and general data and HRCT image characteristics were assessed.

Research results

Among 98 patients, 31 (31.6%) and 67 (68.4%) had mutated and wild-type EGFR in exons 18-21, respectively. Gender, age, smoking history, location of lesions, morphology, edges, borders, pleural indentations, and associations of nodules with bronchus and blood vessels were comparable in both groups (all $P > 0.05$). Patients with mutant EGFR had larger nodules than those with the wild-type (17.19 ± 6.79 and 14.37 ± 6.30 mm, respectively; $P = 0.047$). Meanwhile, the vacuole/honeycomb sign was more frequent in the mutant EGFR group ($P = 0.011$). The logistic regression prediction model included the combination of nodule size and vacuole/honeycomb sign (OR = 1.120, 95%CI: 1.023-1.227, $P = 0.014$) revealed a sensitivity of 83.9%, a specificity of 52.2% and an AUC of 0.698 (95%CI: 0.589-0.806; $P = 0.002$).

Research conclusions

Nodule size and vacuole/honeycomb features could independently predict EGFR mutation status in ground-glass nodular lung adenocarcinoma.

Research perspectives

Future studies are warranted to confirm these findings and improve the non-invasive detection of EGFR gene mutations in lung cancer.

ACKNOWLEDGEMENTS

We immensely thank all the patients for their willingness to share clinical data for research.

REFERENCES

- 1 **Schulze AB**, Evers G, Kerkhoff A. Future Options of Molecular-Targeted Therapy in Small Cell Lung Cancer. *Cancers (Basel)* 2019; **11** pii: E690
- 2 **Travis WD**, Brambilla E, Nicholson AG, Yatabe Y, Austin JHM, Beasley MB, Chirieac LR, Dacic S, Duhig E, Flieder DB, Geisinger K, Hirsch FR, Ishikawa Y, Kerr KM, Noguchi M, Pelosi G, Powell CA, Tsao MS, Wistuba I; WHO Panel. The 2015 World Health Organization Classification of Lung Tumors: Impact of Genetic, Clinical and Radiologic Advances Since the 2004 Classification. *J Thorac Oncol* 2015; **10**: 1243-1260 [PMID: 26291008 DOI: 10.1097/JTO.0000000000000630]
- 3 **Travis WD**. Update on small cell carcinoma and its differentiation from squamous cell carcinoma and other non-small cell carcinomas. *Mod Pathol* 2012; **25** Suppl 1: S18-S30 [PMID: 22214967 DOI: 10.1038/modpathol.2011.150]
- 4 **Rosell R**, Carcereny E, Gervais R, Vergnenegre A, Massuti B, Felip E, Palmero R, Garcia-Gomez R, Pallares C, Sanchez JM, Porta R, Cobo M, Garrido P, Longo F, Moran T, Insa A, De Marinis F, Corre R, Bover I, Illiano A, Dansin E, de Castro J, Milella M, Reguart N, Altavilla G, Jimenez U, Provencio M, Moreno MA, Terrasa J, Muñoz-Langa J, Valdivia J, Isla D, Domine M, Molinier O, Mazieres J, Baize N, Garcia-Campelo R, Robinet G, Rodriguez-Abreu D, Lopez-Vivanco G, Gebbia V, Ferrera-Delgado L, Bombaron P, Bernabe R, Bearz A, Artal A, Cortesi E, Rolfó C, Sanchez-Ronco M, Drozdowskyj A, Queralt C, de Aguirre I, Ramirez JL, Sanchez JJ, Molina MA, Taron M, Paz-Ares L; Spanish Lung Cancer Group in collaboration with Groupe Français de Pneumo-Cancérologie and Associazione Italiana Oncologia Toracica. Erlotinib vs standard chemotherapy as first-line treatment for European patients with advanced EGFR mutation-positive non-small-cell lung cancer (EURTAC): a multicentre, open-label, randomised phase 3 trial. *Lancet Oncol* 2012; **13**: 239-246 [PMID: 22285168 DOI: 10.1016/S1470-2045(11)70393-X]
- 5 **Yang JJ**, Zhou Q, Yan HH, Zhang XC, Chen HJ, Tu HY, Wang Z, Xu CR, Su J, Wang BC, Jiang BY, Bai XY, Zhong WZ, Yang XN, Wu YL. A phase III randomised controlled trial of erlotinib vs gefitinib in advanced non-small cell lung cancer with EGFR mutations. *Br J Cancer* 2017; **116**: 568-574 [PMID: 28103612 DOI: 10.1038/bjc.2016.456]
- 6 **Mok TS**, Wu YL, Thongprasert S, Yang CH, Chu DT, Saijo N, Sunpaweravong P, Han B, Margono B, Ichinose Y, Nishiwaki Y, Ohe Y, Yang JJ, Chewaskulyong B, Jiang H, Duffield EL, Watkins CL, Armour AA, Fukuoka M. Gefitinib or carboplatin-paclitaxel in pulmonary adenocarcinoma. *N Engl J Med* 2009; **361**: 947-957 [PMID: 19692680 DOI: 10.1056/NEJMoa0810699]

- 7 **Hsu WH**, Yang JC, Mok TS, Loong HH. Overview of current systemic management of EGFR-mutant NSCLC. *Ann Oncol* 2018; **29**: i3-i9 [PMID: 29462253 DOI: 10.1093/annonc/mdx702]
- 8 **Passaro A**, Guerini-Rocco E, Pochesci A, Vacirca D, Spitaleri G, Catania CM, Rappa A, Barberis M, de Marinis F. Targeting EGFR T790M mutation in NSCLC: From biology to evaluation and treatment. *Pharmacol Res* 2017; **117**: 406-415 [PMID: 28089942 DOI: 10.1016/j.phrs.2017.01.003]
- 9 **Yatabe Y**, Boreczuk AC, Powell CA. Do all lung adenocarcinomas follow a stepwise progression? *Lung Cancer* 2011; **74**: 7-11 [PMID: 21705107 DOI: 10.1016/j.lungcan.2011.05.021]
- 10 **Jorge SE**, Kobayashi SS, Costa DB. Epidermal growth factor receptor (EGFR) mutations in lung cancer: preclinical and clinical data. *Braz J Med Biol Res* 2014; **47**: 929-939 [PMID: 25296354 DOI: 10.1590/1414-431X20144099]
- 11 **Roviello G**, Zanotti L, Cappelletti MR, Gobbi A, Dester M, Paganini G, Pacifico C, Generali D, Roudi R. Are EGFR tyrosine kinase inhibitors effective in elderly patients with EGFR-mutated non-small cell lung cancer? *Clin Exp Med* 2018; **18**: 15-20 [PMID: 28391544 DOI: 10.1007/s10238-017-0460-7]
- 12 **Cheng Z**, Shan F, Yang Y, Shi Y, Zhang Z. CT characteristics of non-small cell lung cancer with epidermal growth factor receptor mutation: a systematic review and meta-analysis. *BMC Med Imaging* 2017; **17**: 5 [PMID: 28068946 DOI: 10.1186/s12880-016-0175-3]
- 13 **Chan BA**, Hughes BG. Targeted therapy for non-small cell lung cancer: current standards and the promise of the future. *Transl Lung Cancer Res* 2015; **4**: 36-54 [PMID: 25806345 DOI: 10.3978/j.issn.2218-6751.2014.05.01]
- 14 **Diaz LA Jr**, Bardelli A. Liquid biopsies: genotyping circulating tumor DNA. *J Clin Oncol* 2014; **32**: 579-586 [PMID: 24449238 DOI: 10.1200/JCO.2012.45.2011]
- 15 **Zhang H**, Cai W, Wang Y, Liao M, Tian S. CT and clinical characteristics that predict risk of EGFR mutation in non-small cell lung cancer: a systematic review and meta-analysis. *Int J Clin Oncol* 2019
- 16 **Ahmadzada T**, Kao S, Reid G, Boyer M, Mahar A, Cooper WA. An Update on Predictive Biomarkers for Treatment Selection in Non-Small Cell Lung Cancer. *J Clin Med* 2018; **7** [PMID: 29914100 DOI: 10.3390/jcm7060153]
- 17 **Rizzo S**, Petrella F, Buscarino V, De Maria F, Raimondi S, Barberis M, Fumagalli C, Spitaleri G, Rampinelli C, De Marinis F, Spaggiari L, Bellomi M. CT Radiogenomic Characterization of EGFR, K-RAS, and ALK Mutations in Non-Small Cell Lung Cancer. *Eur Radiol* 2016; **26**: 32-42 [PMID: 25956936 DOI: 10.1007/s00330-015-3814-0]
- 18 **Lee HJ**, Kim YT, Kang CH, Zhao B, Tan Y, Schwartz LH, Persigehl T, Jeon YK, Chung DH. Epidermal growth factor receptor mutation in lung adenocarcinomas: relationship with CT characteristics and histologic subtypes. *Radiology* 2013; **268**: 254-264 [PMID: 23468578 DOI: 10.1148/radiol.13112553]
- 19 **Kim HY**, Shim YM, Lee KS, Han J, Yi CA, Kim YK. Persistent pulmonary nodular ground-glass opacity at thin-section CT: histopathologic comparisons. *Radiology* 2007; **245**: 267-275 [PMID: 17885195 DOI: 10.1148/radiol.2451061682]
- 20 **Usuda K**, Sagawa M, Motono N, Ueno M, Tanaka M, Machida Y, Matoba M, Taniguchi M, Tonami H, Ueda Y, Sakuma T. Relationships between EGFR mutation status of lung cancer and preoperative factors - are they predictive? *Asian Pac J Cancer Prev* 2014; **15**: 657-662 [PMID: 24568474 DOI: 10.7314/apjcp.2014.15.2.657]
- 21 **Jang TW**, Oak CH, Chang HK, Suo SJ, Jung MH. EGFR and KRAS mutations in patients with adenocarcinoma of the lung. *Korean J Intern Med* 2009; **24**: 48-54 [PMID: 19270482 DOI: 10.3904/kjim.2009.24.1.43]
- 22 **Naidich DP**, Bankier AA, MacMahon H, Schaefer-Prokop CM, Pistolesi M, Goo JM, Macchiarini P, Crapo JD, Herold CJ, Austin JH, Travis WD. Recommendations for the management of subsolid pulmonary nodules detected at CT: a statement from the Fleischner Society. *Radiology* 2013; **266**: 304-317 [PMID: 23070270 DOI: 10.1148/radiol.12120628]
- 23 **Hasegawa M**, Sakai F, Ishikawa R, Kimura F, Ishida H, Kobayashi K. CT Features of Epidermal Growth Factor Receptor-Mutated Adenocarcinoma of the Lung: Comparison with Nonmutated Adenocarcinoma. *J Thorac Oncol* 2016; **11**: 819-826 [PMID: 26917231 DOI: 10.1016/j.jtho.2016.02.010]
- 24 **Yano M**, Sasaki H, Kobayashi Y, Yukiue H, Haneda H, Suzuki E, Endo K, Kawano O, Hara M, Fujii Y. Epidermal growth factor receptor gene mutation and computed tomographic findings in peripheral pulmonary adenocarcinoma. *J Thorac Oncol* 2006; **1**: 413-416 [PMID: 17409892]
- 25 **Dai J**, Shi J, Soodeen-Laloo AK, Zhang P, Yang Y, Wu C, Jiang S, Jia X, Fei K, Jianga G. Air bronchogram: A potential indicator of epidermal growth factor receptor mutation in pulmonary subsolid nodules. *Lung Cancer* 2016; **22**-28
- 26 **Han X**, Zhang Z, Wu D, Shen Y, Wang S, Wang L, Liu Y, Yang S, Hu X, Feng Y, Sun Y, Shi Y. Suitability of surgical tumor tissues, biopsy, or cytology samples for epidermal growth factor receptor mutation testing in non-small cell lung carcinoma based on chinese population. *Transl Oncol* 2014; **7**: 795-799 [PMID: 25500090 DOI: 10.1016/j.tranon.2014.10.008]
- 27 **Lee SM**, Bae SK, Jung SJ, Kim CK. FDG uptake in non-small cell lung cancer is not an independent predictor of EGFR or KRAS mutation status: a retrospective analysis of 206 patients. *Clin Nucl Med* 2015; **40**: 950-958 [PMID: 26359571 DOI: 10.1097/rlu.0000000000000975]
- 28 **Liu Y**, Kim J, Qu F, Liu S, Wang H, Balagurunathan Y, Ye Z, Gillies RJ. CT Features Associated with Epidermal Growth Factor Receptor Mutation Status in Patients with Lung Adenocarcinoma. *Radiology* 2016; **280**: 271-280 [PMID: 26937803 DOI: 10.1148/radiol.2016151455]

- 29 **Hong SJ**, Kim TJ, Choi YW, Park JS, Chung JH, Lee KW. Radiogenomic correlation in lung adenocarcinoma with epidermal growth factor receptor mutations: Imaging features and histological subtypes. *Eur Radiol* 2016; **26**: 3660-3668 [PMID: [26787602](#) DOI: [10.1007/s00330-015-4196-z](#)]
- 30 **Oda S**, Awai K, Liu D, Nakaura T, Yanaga Y, Nomori H, Yamashita Y. Ground-glass opacities on thin-section helical CT: differentiation between bronchioloalveolar carcinoma and atypical adenomatous hyperplasia. *AJR Am J Roentgenol* 2008; **190**: 1363-1368 [PMID: [18430856](#) DOI: [10.2214/ajr.07.3101](#)]
- 31 **Song YS**, Park CM, Park SJ, Lee SM, Jeon YK, Goo JM. Volume and mass doubling times of persistent pulmonary subsolid nodules detected in patients without known malignancy. *Radiology* 2014; **273**: 276
- 32 **Park S**, Lee SM, Kim S, Lee JG, Seo JB. Volume Doubling Times of Lung Adenocarcinomas: Correlation with Predominant Histologic Subtypes and Prognosis. *Radiology* 2020; **295**: 191835
- 33 **Potter AL**, Bajaj SS, Yang CJ. The 2021 USPSTF lung cancer screening guidelines: a new frontier. *Lancet Respir Med* 2021; **9**: 689-691 [PMID: [33965004](#) DOI: [10.1016/S2213-2600\(21\)00210-1](#)]
- 34 **Canadian Task Force on Preventive Health Care**. Recommendations on screening for lung cancer. *CMAJ* 2016; **188**: 425-432 [PMID: [26952527](#) DOI: [10.1503/cmaj.151421](#)]
- 35 **NCCN Clinical Practice Guidelines in Oncology**. Lung Cancer Screening. Version 2.2021. Fortg Washington: National Comprehensive Cancer Network, 2020



Published by **Baishideng Publishing Group Inc**
7041 Koll Center Parkway, Suite 160, Pleasanton, CA 94566, USA
Telephone: +1-925-3991568
E-mail: bpgoffice@wjgnet.com
Help Desk: <https://www.f6publishing.com/helpdesk>
<https://www.wjgnet.com>

